Pairing collectivity in medium-mass neutron-rich nuclei near drip-line *

M. Matsuo[a], Y. Serizawa[a], and K. Mizuyama[a]

[a]Department of Physics, Faculty of Science Niigata University, Niigata 950-2181, Japan

We look for collective excitations originating from the strong surface pairing in unstable nuclei near the neutron drip-line. The soft dipole excitation is such a pairing mode as it exhibits a character of core-vs-dineutron motion. Possibility of the hydrodynamic phonon mode (the Anderson-Bogoliubov mode) is also discussed.

1. Introduction

The pair correlation is known to play central roles in characterizing various structure aspects of nuclei[1]. As far as nuclei near the stability line are concerned, the energy scale of the correlation, the pair gap $\Delta \sim 1-2$ MeV, is much smaller than the other fundamental energy scales, the Fermi energy $e_F \sim 40$ MeV, the shell gap $\sim$ several MeV and the nucleon separation energy ~ 8 MeV. This situation can be regarded as that of the weak coupling pairing to which the conventional BCS models can be successfully applied. The correlated nucleon pair in this case is reasonably described as a pair coupled to the total angular momentum $I = 0$ consisting of a small number of single-particle j-shell orbits around the Fermi energy.

Unstable nuclei near the neutron drip-line are in a very different situation. The neutron separation energy becomes comparable with or even smaller than the typical pair gap. The single-particle shell tends to lose its sense since the continuum orbits take part in. Moreover neutrons in the low density external region associated with skin and/or halo feel stronger n-n attraction due to the momentum dependence of the nuclear force. One can expect then that the pair correlation in this 'extreme' condition may differ from that in stable nuclei. An important clue is the di-neutron correlation (the spatially compact correlated neutron pair), which has been investigated intensively for light two-neutron halo nuclei ^{11}Li and ^{6}He[2, 3, 4, 5, 6, 7, 8, 9]. In addition our previous study suggests that the di-neutron correlation persists also in medium-mass neutron-rich nuclei containing more than two weakly bound neutrons[10].

In this presentation, we first demonstrate, by using a calculation for uniform neutron matter[11], that the di-neutron correlation is naturally expected in low density region. We shall interprete the di-neutron correlation in terms of the BCS-BEC crossover[12, 13, 14, 15] which takes place in between the weak coupling pairing of the conventional BCS theory and the strong coupling pairing leading to a Bose-Einstein condensate of correlated pairs. In other words, the di-neutron correlation is an signature of the strong coupling

*This work was supported by the Grant-in-Aid for Scientific Research (No. 17540244) from the Japan Society for the Promotion of Science.

pairing. If the strong coupling pairing is the case, it will influence excitation properties of nuclei. This is the issue which we discuss in the latter half of the presentation. We look for another manifestation of the strong coupling pairing by analyzing dipole and quadrupole responses of medium-mass neutron-rich nuclei.

2. Low density uniform matter and the BCS-BEC crossover

Let us discuss properties of the neutron pair correlation in uniform neutron matter at low density[11]. We employ results of the BCS approximation applied to the bare nuclear force. The G3RS force is adopted, and the effective mass consistent with the Gogny Hartree-Fock is used. The calculation itself is essentially the same as other BCS calculations using the bare forces [1].

Within this scheme the gap and the number equations can be solved exactly by a numerical method as a function of neutron density $\rho = k_F^3/3\pi^2$, where k_F is the Fermi momentum. We can analyze spatial structure of the pair correlation by means of the wave function of the correlated neutron pair (the Cooper pair), which is given by

$$\Psi_{pair}(r) \propto \langle \Phi_0 | \, \psi^\dagger(\boldsymbol{r}' + \boldsymbol{r}/2 \uparrow)\psi^\dagger(\boldsymbol{r}' - \boldsymbol{r}/2 \downarrow) \, |\Phi_0\rangle = \frac{1}{(2\pi)^3} \int d\boldsymbol{k} u_k v_k e^{i\boldsymbol{k}\cdot\boldsymbol{r}} \tag{1}$$

where u_k, v_k are the u,v-factors in the momentum representations. As a measure of the spatial structure, the r.m.s. radius of the Cooper pair or the coherence length

$$\xi = \sqrt{\langle r^2 \rangle}, \qquad \left\langle r^2 \right\rangle = \int d\boldsymbol{r} r^2 |\Psi_{pair}(r)|^2 \tag{2}$$

is evaluated from the Cooper pair wave function.

Fig.1 shows examples of the neutron Cooper pair wave function (its square modulus $r^2|\Psi(r)|^2$) in neutron matter at the density ρ/ρ_0 =1, 1/2, 1/8 and 1/64 (ρ_0 being the neutron density in the normal nuclear matter given by $\rho_0 = k_{F,0}^3/3\pi^2$ with $k_{F,0} = 1.36$ fm^{-1}). The pair gap Δ evaluated at the Fermi energy and the coherence length ξ are also shown in the figure. An important observation is that the size of the neutron Cooper pair is as small as $\xi \sim 5$ fm at the low density $\rho/\rho_0 = 1/8 - 1/64$. This is in contrast to the cases around the normal density $\rho/\rho_0 = 1 - 1/2$ where the coherence length becomes considerably large $\xi \gtrsim 10^1$fm. It is seen in Fig.1 that the profile of the Cooper pair wave function also varies significantly with the density. At the density $\rho/\rho_0 = 1/8 - 1/64$, the profile resembles to that of a bound state wave function in free space while the wave function at the normal density deviates significantly from that of the free-space bound state.

Implications of the spatial di-neutron correlation at the low density can be clarified by considering a possible link to the BCS-BEC crossover[12, 13, 14, 15]. The crossover is a general phenomenon which occurs in superfluid/superconducting Fermion systems as the attractive interaction among the partner Fermions is varied from the weak to strong cases. The crossover has been observed recently in an ultra cold Fermion gas in a trap[16]. The weak coupling case corresponds to the conventional electron superconductivity in metals, and it is often called the weak coupling BCS since it is the situation assumed in the original BCS theories. In this case, the pair gap Δ is much smaller than the Fermi energy e_F, and the coherence length ξ (the size of the Cooper pair) is much larger than

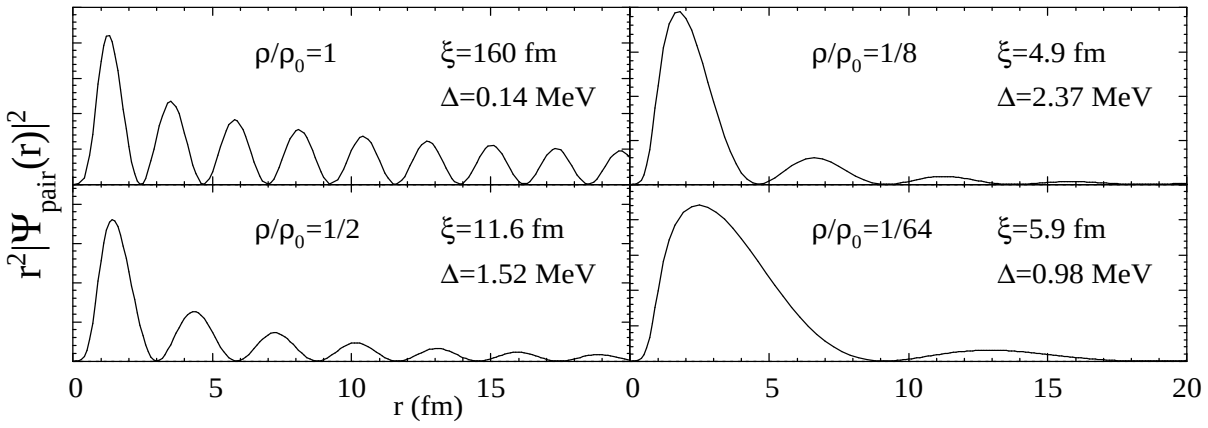

Figure 1. The probability distribution $r^2|\Psi_{pair}(r)|^2$ of the wave function of a neutron Cooper pair in low density neutron matter. The horizontal axis is the relative coordinate r between the partner neutrons.

the average inter-particle distance $d = \rho^{-1/3} = 3.09k_F^{-1}$. If the attraction among the pair partners becomes stronger (the pair gap gets larger accordingly), the ratio Δ/e_F between the pair gap and the Fermi energy increases monotonically, and the ratio ξ/d between the coherence length and the average inter-particle distance decreases. In the limit of strong coupling, the Cooper pair coincides with the bound Fermion pair in free space. The system is then a Bose-Einstein condensate (BEC) of the bound pairs. The transition, though gradual in nature, from the weak coupling BCS to the strong coupling BEC occurs around $\Delta/e_F \sim 1$ and $\xi/d \sim 1$. Reference values for the two ratios characterizing the BCS-BEC crossover are[15]; $\Delta/e_F = 0.21$ and $\xi/d = 1.10$ for the boundary to the weak coupling BCS, $\Delta/e_F = 1.33$ and $\xi/d = 0.19$ for the boundary to the strong coupling BEC, and $\Delta/e_F = 0.69$ and $\xi/d = 0.36$ for the unitarity limit corresponding to the midway of the crossover.

In Fig.2 ploted are the ratios Δ/e_F and ξ/d calculated for neutron matter. Two important features are seen. Firstly the ratios strongly vary with the neutron density, in particular in the range $\rho/\rho_0 = 1 - 10^{-1}$. Secondly the two ratios both indicate that the system enters the regime of the BCS-BEC crossover at low density in a wide range $\rho/\rho_0 \sim 10^{-1} - 10^{-4}$. A strong di-neutron correlation is obvious since the size of the neutron Cooper pair ξ is smaller than the average inter-neutron distance d. It should be noted that the strong variation as a function of the density arises from the fact that the ^1S interaction matrix element or the scattering T-matrix has strong momentum dependence.

3. Pairing collectivity in neutron-rich nuclei

3.1. Skyrme-HFB plus continuum QRPA approach

We shall now discuss the pair correlation in neutron-rich nuclei in the medium-mass region. We shall focus on the role of the pair correlation in collective responses. For this purpose we employ the selfconsistent Hartree-Fock-Bogoliubov approach to describe the ground state and the static mean-fields[17], and we also use the continuum QRPA

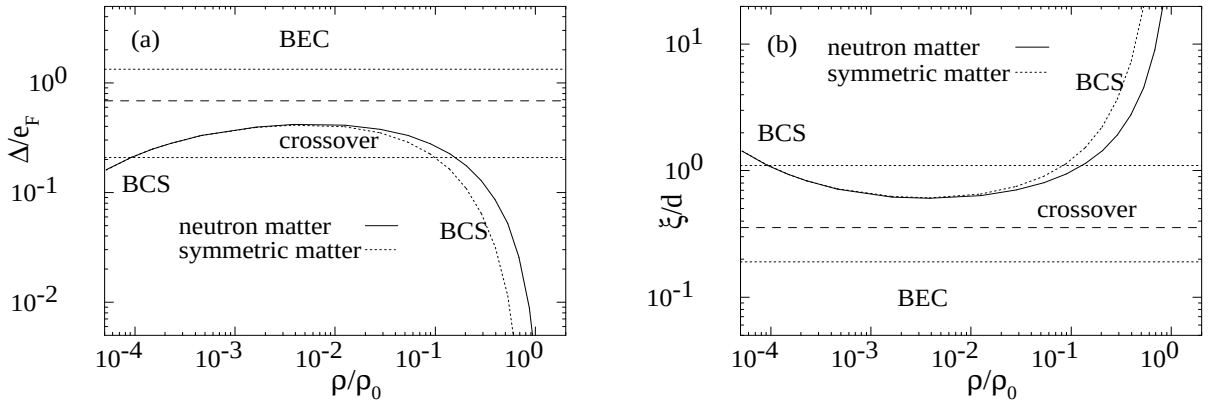

Figure 2. (a) The ratio Δ/e_F between the pair gap Δ and the Fermi energy e_F as a function of the neutron density in uniform neutron matter. The boundaries characterizing the BCS-BEC crossover are drawn by horizontal dotted and dashed lines. The dotted curve is the ratio for uniform symmetric matter. (b) The same as (a) but for the ratio ξ/d between the coherence length ξ and the average inter-neutron distance d.

method to describe the response[10, 18]. In the following, we present results for ^{120}Sn representative of stable nuclei, and those for ^{158}Sn, in which the neutron separation energy is as small as $\sim$1 MeV.

The Skyrme effective interaction with the SLy4 parameter set is used. As the effective interaction responsible for pairing, we use a density-dependent delta interaction (DDDI) of the form $v(\boldsymbol{r}-\boldsymbol{r}') = V_{0,\tau}[\rho(\boldsymbol{r})]\delta(\boldsymbol{r}-\boldsymbol{r}')$, where the density dependent interaction strength is given by

$$V_{0,\tau}[\rho(\boldsymbol{r})] = v_0\left(1-\eta\left(\frac{\rho_\tau(\boldsymbol{r})}{\rho_c}\right)^\alpha\right), \quad (\tau = n,p), \quad \rho_c = 0.08 \text{ fm}^{-3}. \tag{3}$$

Here the overall force constant $v_0 = -458.4$MeV fm^{-3} is fixed to reproduce the ^1S scattering length $a = -18$fm in free space. The density dependence factor of the interaction enables us to simulate the momentum dependence of the bare nucleon force. Applying the DDDI to uniform matter, we determine the remaining parameters as $\eta = 0.845$ and $\alpha = 0.59$, and also the cut-off quasiparticle energy ($E_{cut} = 60$ MeV) so that the DDDI reproduces the pair gap Δ and the coherence length ξ obtained from the bare force[11]. Direct application of this parameter set to finite nuclei, however, gives a gap smaller than the experimental values.

If we change the parameter η, it is possible to control the effective pairing interaction without changing the scattering length in free space outside the nuclear surface. A smaller value of η, i.e., weaker density dependence, gives stronger pairing interaction inside the nucleus. We find that $\eta = 0.71$ gives an average pair gap which is comparable to the experimental value $\Delta \sim 1.1 - 1.4$ MeV in stable Sn isotopes. If we adopt smaller values of η, the pair gap is further enhanced. Figure 3 shows the calculated pair potential $\Delta(r)$ for various choices of η. The case $\eta = 0$, implying a density-independent delta interaction constrained only by the scattering length, leads to an extremely large pair

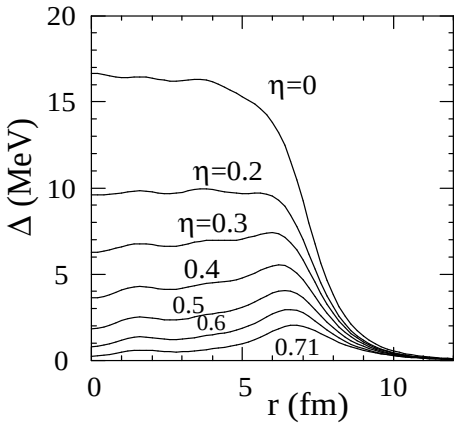

Figure 3. The neutron pair potential $\Delta(r)$ calculated for ^{158}Sn with use of various values of the parameter η of the density-dependent delta interaction.

potential $\Delta(r) \sim 15$ MeV. This value of the pair potential is of course too large compared to the reality. However we exploit this feature in order to explore what properties could emerge if the strong coupling pairing dominates in the whole nuclear volume.

As the residual interaction to be used in the continuum QRPA calculation, we use the same DDDI for the pairing channel while the Landau-Migdal approximation to the Skyrme interaction is used for the particle-hole channel. We introduce a renormalization factor to the particle-hole residual interaction so that a spurious center-of-mass mode is placed at the zero-energy.

3.2. Anderson-Bogoliubov mode associated with strong pairing

Let us first consider the extreme limit of the strong pairing ($\eta = 0$ and $\Delta \sim 15$ MeV) in the stable nucleus ^{120}Sn. What kinds of collective mode can be expected in such a case?

The solid curve in Fig.4(a) shows the E1 strength function in this case. A remarkable feature is that a very sharp resonance emerges at $E \sim 14$ MeV. This is quite different from the widely spread strength distribution, the giant dipole resonance, in the case of the normal pairing $\eta = 0.71$ and $\Delta \sim 1-2$ MeV (the dotted curve in Fig.4(a)). The transition densities for this sharp resonance (Fig.4(b)) are indeed very different from those of the isovector giant dipole resonance. The largest difference is that the particle-pair transition density $\delta\langle\psi^\dagger\psi^\dagger\rangle$ and the hole-pair transition density $\delta\langle\psi\psi\rangle$ are much larger than the particle-hole transition density $\delta\langle\psi^\dagger\psi\rangle$. This indicates that the mode is characterized by an oscillation of the pair potential $\Delta(\boldsymbol{r})$, and hence it is a collective mode associated with the pairing degrees of freedom. The opposite sign between $\delta\langle\psi^\dagger\psi^\dagger\rangle$ and $\delta\langle\psi\psi\rangle$ indicates that the mode accompanies an oscillation in the phase of the pair potential $\Delta(\boldsymbol{r})$.

The collective mode associated with the phase of the pair potential $\Delta(\boldsymbol{r})$ is known as the Anderson-Bogoliubov mode [19, 20, 21]. In uniform superfluid neutral Fermions, the Anderson-Bogoliubov mode is a collective hydrodynamic phonon mode with the dispersion relation $\omega = cq$, where the sound velocity is given by $c \approx v_F/\sqrt{3}$, and q and ω are the momentum and the frequency of the phonon mode. The phase oscillation couples to density oscillation for $q > 0$, and hence it causes hydrodynamic motion of the superfluid. It is seen in Fig.4(b) that the radial profile of the calculated transition densities is very much similar to the Bessel function $j_l(kr)$, a typical feature of hydrodynamic motion in a spherical system. This indicates that the sharp resonance is a nuclear Anderson-

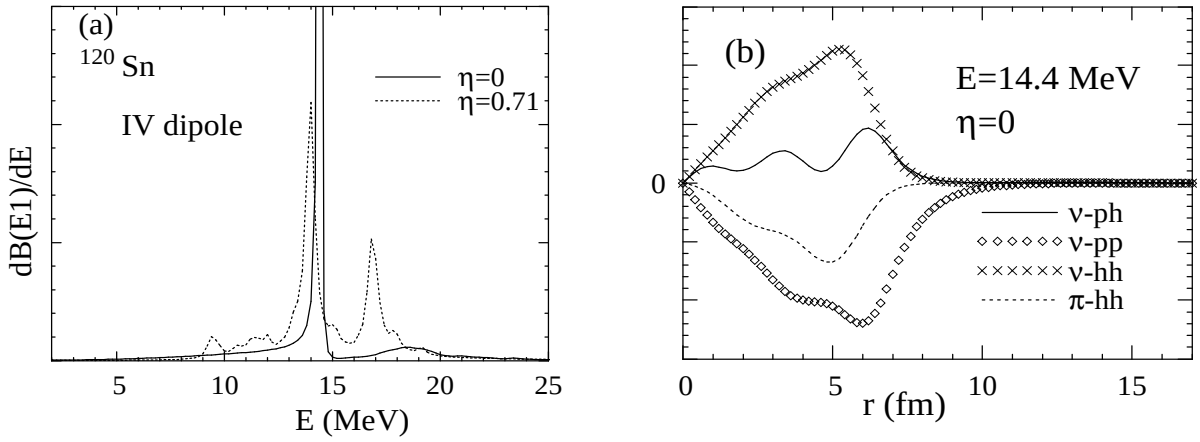

Figure 4. (a) The E1 strength function in ^{120}Sn calculated using the normal pairing ($\eta = 0.71$, the dotted curve) and the one using the strong pairing ($\eta = 0$, the solid curve). (b) The transitions densities associated with the sharp peak at $E = 14.4$ MeV for the strong pairing ($\eta = 0$). The neutron particle-hole transition density $\delta\langle\psi^\dagger(\boldsymbol{r}\sigma)\psi(\boldsymbol{r}\sigma)\rangle$ ($\nu-$ph) , the neutron particle-pair transition density $\delta\langle\psi^\dagger(\boldsymbol{r}\uparrow)\psi^\dagger(\boldsymbol{r}\downarrow)\rangle$ ($\nu-$pp), the neutron hole-pair transition density $\delta\langle\psi(\boldsymbol{r}\uparrow)\psi(\boldsymbol{r}\downarrow)\rangle$ ($\nu-$hh), and the proton particle-hole density ($\pi-$ph) are plotted.

Bogoliubov mode. It is also seen in Fig.4(b) that the transition densities for neutrons and protons have opposite phase. This mode is therefore interpreted as an Anderson-Bogoliubov mode consisting of two kinds of superfluid oscillating with opposite phase. (Because of the presence of two fluids, it differs from an Anderson-Bogoliubov mode in a trapped superfluid Fermion gas[22, 23].)

It should be remarked here that the features of the Anderson-Bogoliubov mode is not seen clearly at weaker pairing. In the cases of $\Delta \sim 3$ MeV ($\eta = 0.5$) and 1-2 MeV ($\eta = 0.71$) the transition densities of the high-lying resonance (not shown here) are characterized not by the Anderson-Bogoliubov mode, but rather by the usual giant dipole response where the pair transition densities play only minor roles.

3.3. Core-vs-dineutron mode in nuclei near the drip-line

An important question is how the dipole response changes if we consider neutron-rich nuclei near the drip line. Figure 5(a) shows the E1 strength distribution in ^{158}Sn for various values of η, covering from the normal pairing case ($\Delta = 1 - 2$MeV, $\eta = 0.71$) to the strong pairing case ($\Delta \sim 15$MeV, $\eta = 0$). The strength distribution in ^{158}Sn and those in ^{120}Sn (Fig.4(a)) are quite different both in the case of the normal pairing and in the case of the strong pairing. In the normal pairing case ($\eta = 0.71$), the strength function exhibits a large low-lying bump around $E = 2 - 8$ MeV (the soft dipole excitation) beside the high-lying resonance ($E = 10 - 18$ MeV, the giant dipole resonance). It appears that, with increasing the pair correlation, the strength of the low-lying bump develops, and simultaneously the giant resonance changes its structure. In the strong pairing case ($\eta = 0$), the dipole strength function exhibits a broad peak around $E = 5 - 15$ MeV.

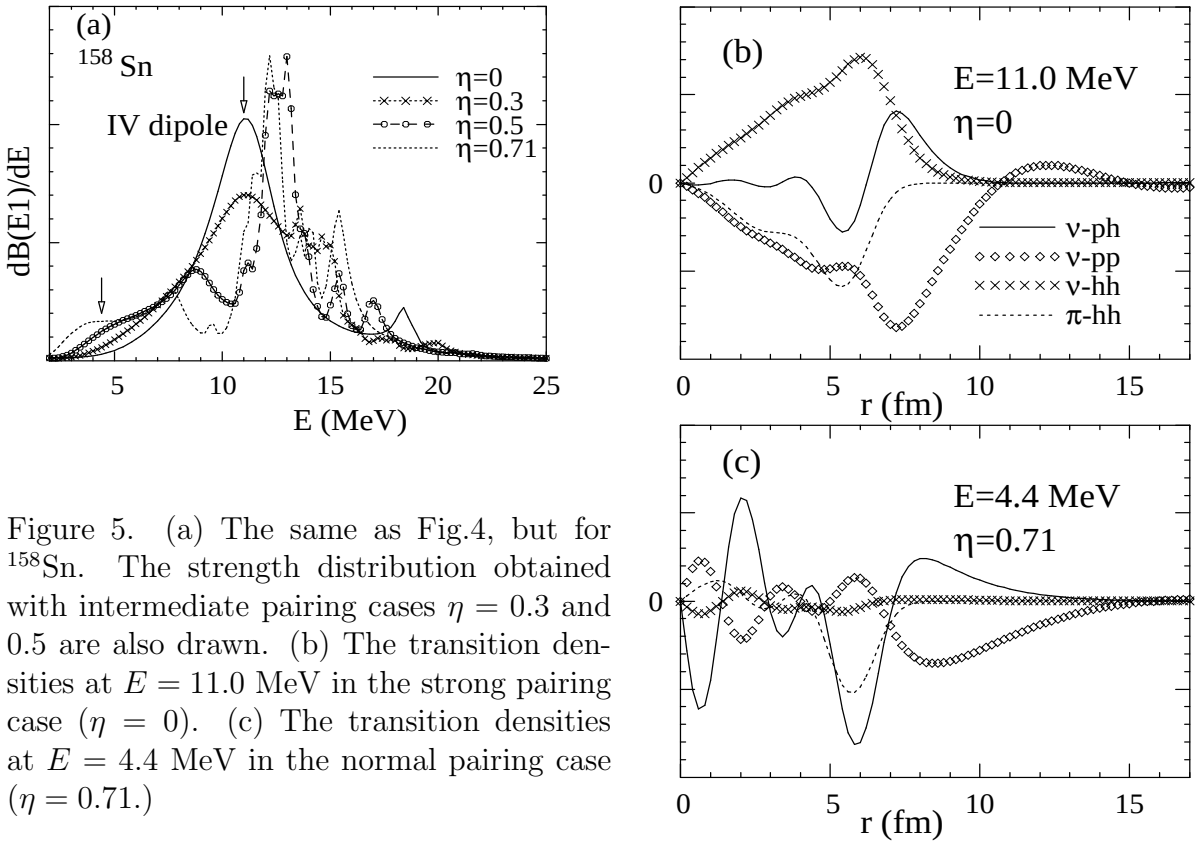

Figure 5. (a) The same as Fig.4, but for ^{158}Sn. The strength distribution obtained with intermediate pairing cases $\eta = 0.3$ and 0.5 are also drawn. (b) The transition densities at $E = 11.0$ MeV in the strong pairing case ($\eta = 0$). (c) The transition densities at $E = 4.4$ MeV in the normal pairing case ($\eta = 0.71$.)

To identify the characters of the dipole modes, we plot in Fig.5(b) the transition densities at the broad peak emerging in the strong pairing case ($\eta = 0, \Delta \sim 15$ MeV). A clear difference from that of ^{120}Sn (Fig.4(b)) is seen in behaviors around the nuclear surface and in the external region. In the case of ^{158}Sn, the particle-hole transition density for neutrons (the solid curve in Fig.5(b)) has a node at a position near the nuclear surface. Just inside this node, neutrons and protons move with the same phase while in the external region neutron motion is dominating. This feature indicates that neutrons in the external region move against the dipole motion of the core. It is also noted that the neutron-pair transition density (ν-pp) has the largest amplitude in the external region, and it exhibits oscillation far outside the surface. This can be interpreted as being caused by motion of the di-neutrons (a core-vs-dineutron motion), which accompanies significant escaping of di-neutrons from the excitated states[10].

As far as the internal region is concerned, on the other hand, the transition densities exhibit the typical features of the Anderson-Bogoliubov mode found in Fig.4(b). The broad peak around $E = 5 - 15$ MeV in the strong pairing case has a character of a mixture of the Anderson-Bogoliubov mode and the core-vs-dineutron mode.

Fig.5(c) is the transition densities for the soft-dipole excitation seen in the normal pairing case. Focusing on the properties around the surface and in the external region, we notice that both Fig.5(b) and (c) exhibit a character of the core-vs-dineutron motion. Combining resutls for intermediate pairing strengths $\eta = 0.3$, and 0.5 (not shown here), we find that the core-vs-dineutron mode is always present in the low-lying part of the

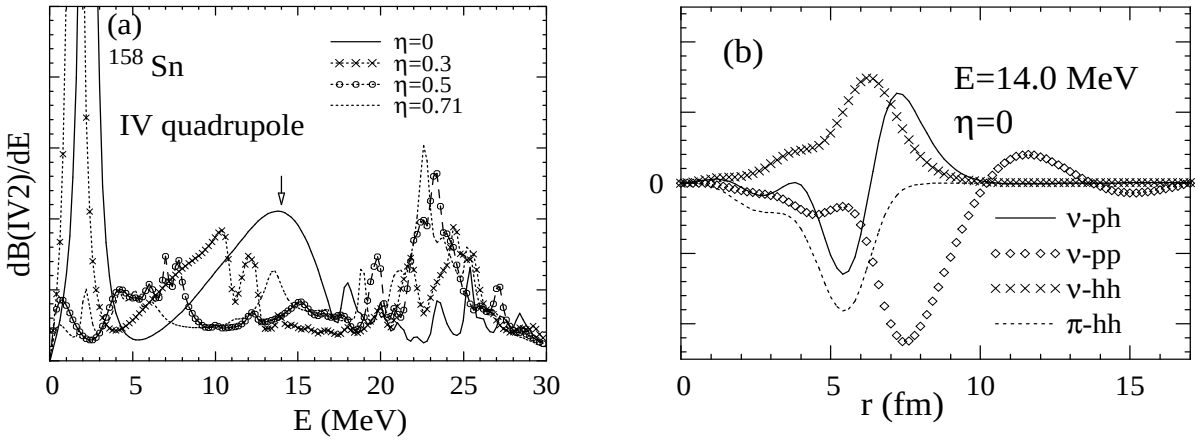

Figure 6. (a) The same as Fig.5(a), but for the quadrupole response. (b) The transition densities evaluated at the energy $E = 14.0$ MeV in the case of strong pairing ($\eta = 0$).

dipole strength distribution in the whole considered range $\eta = 0 - 0.71$ of the parameter η. This is quite in contrast to the fact that the Anderson-Bogoliubov mode emerges only at the very strong pairing $\Delta > 7$ MeV.

3.4. Quadrupole core-vs-dineutron mode

Fig.6(a) shows the isovector quadrupole response of ^{158}Sn for various pairing strengths. There are three peaks/bump in the strength distribution. The peak around $E \sim 20 - 27$ MeV is the isovector GQR. The IV-GQR tends to diminish if the pairing strength is increased to $\Delta \gtrsim 7$ MeV. It is noticed that a low-lying bump around $E = 5 - 17$ MeV emerges only when the pairing is taken stronger ($\Delta > 3$ MeV, $\eta < 0.5$). (The third peak, the sharp one around $E \sim 2$ MeV is the surface oscillation having an isoscalar character.) The transition densities of this low-lying bump for the strongest pairing $\eta = 0$ $\Delta \sim 15$ MeV is shown in Fig.6(b). The profile is similar to those of Fig.5(b)(c) in the surface and in the external region, and hence this mode is also interpreted as the core-vs-dineutron mode. Noting the fact that the core-vs-dineutron mode emerges both in the dipole and quadrupole responses, we consider that the core-vs-dineutron mode is a fundamental mode of excitation in superfluid nuclei near the neutron drip-line. In the quadrupole case, however, the low-lying core-vs-dineutron mode emerges only in the unrealistically strong pairing cases $\Delta \gtrsim 3$ MeV while in the dipole case it is present even with the realistic pairing. This difference is due to the shell effect.

4. Conclusions

The spatial di-neutron correlation is closely related to the pair correlation in the strong coupling regime. The neutron pairing in low density uniform matter approaches to this situation in a wide density range $\rho/\rho_0 \sim 10^{-1} - 10^{-4}$. The concept of BCS-BEC crossover is useful to characterize this behavior.

We have discussed how the strong coupling pairing inluences collective excitations in medium-mass neutron-rich nuclei. To obtain an overall picture, we have varied artificially

the effective pairing interaction so that we can cover not only a realistic situation, where the strong coupling pairing is expected only in the surface region with low density, but also an extreme limit where the strong coupling prevails in the whole density range and in the whole nuclear volume.

We found that there are two kinds of collective excitation associated with the strong coupling pairing. The first is the Anderson-Bogoliubov phonon mode, which is essentially an hydrodynamic motion of two kinds of superfluid with an isovector character. However, this emerges only if an unrealistically strong pairing interaction is used. The second is the core-vs-dineutron mode taking place around the nuclear surface. It shows up in nuclei near the neutron drip-line even for the realistic pairing interaction with reasonable density-dependence. It is nothing but the soft dipole excitation. The soft dipole excitation is an important clue to study the strong surface pairing in nuclei near the drip-line.

REFERENCES

1. D. J. Dean and M. Hjorth-Jensen, Rev. Mod. Phys. 75 (2003) 607, and references therein.
2. T. Nakamura, et.al., Phys. Rev. Lett. 96 (2006) 252502.
3. P. G. Hansen and B. Jonson, Europhys. Lett. **4** (1987) 409.
4. G. F. Bertsch and H. Esbensen, Ann. Phys. **209**, 327 (1991).
5. K. Ikeda, Nucl. Phys. A538 (1992) 355c.
6. M. V. Zhukov, et.al., Phys. Rep. 231 (1993) 151.
7. F. Barranco, et.al., Eur. Phys. J. A11 (2001) 385.
8. T. Myo, S. Aoyama, K. Katō, and K. Ikeda, Phys. Lett. B576 (2003) 281.
9. K. Hagino and H. Sagawa, Phys. Rev. C 72 (2005) 044321.
10. M. Matsuo, K. Mizuyama, and Y. Serizawa, Phys. Rev. C 71 (2005) 064326.
11. M. Matsuo, Phys. Rev. C 73 (2006) 044309.
12. A. J. Leggett, in *Modern Trends in the Theory of Condensed Matter*, Lecture Note in Physics 115, ed. by A. Pekalski and R. Przystawa (Springer-Verlag, Berlin, 1980); J. de Phys. 41 (1980) C7-19.
13. P. Nozières and S. Schmitt-Rink, J. Low Temp. Phys. 59 (1985) 195.
14. M. Randeria, in *Bose-Einstein Condensation*, ed. by A. Griffin, D. Snoke, and S. Stringari (Cambridge Univ. Press, Cambridge, 1995).
15. J. R. Engelbrecht, M. Randeria, and C. A. R. Sá de Melo, Phys. Rev. B 55 (1997) 15153.
16. C. A. Regal, M. Greiner, and D. S. Jin, Phys. Rev. Lett. 92 (2004) 040403.
17. J. Dobaczewski, H. Flocard, and J. Treiner, Nucl. Phys. A422 (1984) 103.
18. M. Matsuo, Nucl. Phys. A696 (2001) 371.
19. P. W. Anderson, Phys. Rev. 112 (1958) 1900.
20. N. N. Bogoliubov, V. V. Tolmachev, D. V. Shirkov, *A New Method in the Theory of Superconductivity*, (Academy of Science, Moskow 1958).
21. V. M. Galitskii, JETP 34 (1958) 1011.
22. M. A. Baranov and D. S. Petrov, Phys. Rev. A 62 (2000) 041601(R).
23. G. M. Bruun and B. R. Mottelson, Phys. Rev. Lett. 87 (2001) 270403.